Received: 24 May 2019 | Revised: 14 July 2020 | Accepted: 22 September 2020

DOI: 10.1002/eqe.3370

WILEY

RESEARCH ARTICLE

Variance-based sensitivity analyses and uncertainty quantification for FEMA P-58 consequence predictions

Gemma Cremen[1] | **Jack W. Baker**[2]

[1] Department of Civil, Environmental and Geomatic Engineering, University College London, London, UK

[2] Department of Civil and Environmental Engineering, Stanford University, California

Correspondence:
Gemma Cremen, Department of Civil, Environmental and Geomatic Engineering, Chadwick Building, University College London, Gower Street, London WC1E 6BT, UK.
Email: g.cremen@ucl.ac.uk

Abstract

Earthquake loss assessment procedures for individual buildings can be a useful tool for various stakeholders, including building owners, insurers, and lenders. However, it is often not possible to provide complete information for the required inputs to these procedures because there is substantial cost and effort associated with gathering necessary data. It is therefore important to understand how different inputs to these procedures (building information/ground shaking intensity) impact the loss predictions. This can be done via sensitivity analyses. We conduct variance-based sensitivity analyses for the FEMA P-58 methodology, a building-specific seismic performance assessment procedure that is making its way into seismic design and risk analysis practice. We determine how variations in different input variables of the methodology affect predictions of building loss ratio and reoccupancy time, and benchmark calculated sensitivities using the HAZUS earthquake loss estimation methodology . We also quantify additional uncertainty in consequence predictions caused by uncertainty in input variables. We use an example site in downtown Los Angeles and consider a 7-story and a 14-story building. Of the six inputs considered in the analyses, building loss ratio predictions are most sensitive to shaking intensity and building age, while reoccupancy time predictions are most sensitive to shaking intensity and the type of lateral system/building period. The largest additional uncertainties in building loss ratio predictions are caused by the building's lateral system or age (or both) being unknown. The results of this study provide an enhanced understanding of the interaction between inputs and consequence predictions of the P-58 methodology.

KEYWORDS

FEMA P-58 methodology, seismic loss predictions, sensitivity analysis, uncertainty quantification

1 | INTRODUCTION

The prediction of earthquake-induced loss is important for a number of different stakeholders including building owners, emergency planners, the insurance and reinsurance industries, and local and national governments.[1] For example,

calculations of probable maximum loss (PML), which is the probable cost of repairing earthquake damage with a given confidence of nonexceedance in a particular earthquake return period, are used to determine insurance premiums, prepare disaster response plans, create land-use zoning policies, and develop building codes.[2] Commercial lenders also often use PML to help decide whether to underwrite a mortgage in seismically active regions; it is common for such lenders to require the buyer to purchase earthquake insurance for a mortgage to be issued if the PML exceeds 20–30% of the building's replacement cost.[3]

These loss calculations can be conducted with crude and incomplete building information, however.[4,5] For example, in the catastrophe insurance industry, many insurers provide incomplete information on even basic characteristics, such as location and occupancy type.[6] In addition, there is often limited availability of data to fully characterize the events of interest.[7] It is therefore important to understand how uncertainties in inputs to seismic loss models for individual buildings can affect the loss predictions,[8] which can be useful for many applications, e.g., insuring supply-chain risk. Several previous studies have investigated the sensitivity of building-specific seismic loss procedures to different model inputs. Dyanati et al[9] examined the impact of ground motion and structural response calculations on expected annual dollar losses for a six-story braced frame building. Lamprou et al[10] estimated the effect of uncertain parameters associated with seismic hazard and component-level damage on expected life-cycle seismic repair costs for a four-story concrete moment-frame building. Finally, Porter et al[11] evaluated the relative contribution of various ground motion, building, and economic parameters to overall seismic performance (i.e., repair cost) uncertainty for a 1960s high-rise nonductile moment-frame building.

In this study, we conduct sensitivity analyses of the FEMA P-58 methodology, which is making its way into seismic design and risk analysis practice. FEMA P-58 is a building-specific seismic performance assessment procedure,[12] based on the performance-based earthquake engineering philosophy.[13] It combines ground motion hazard, structural response, and component-level damage to make predictions of loss induced by earthquake loading. The methodology is probabilistic in nature, employing Monte Carlo sampling at each stage in the analysis to capture uncertainties. Using a 7-story and a 14-story building in downtown Los Angeles as case studies, we investigate how different input parameters affect various loss predictions. We benchmark results of the sensitivity analyses using the HAZUS earthquake loss estimation methodology. We also quantify additional uncertainties in losses that result due to uncertain model inputs.

Our analyses significantly differ from the calculations of the aforementioned previous studies for several reasons. First, we examine the sensitivity of more fundamental input parameters, such as lateral system type and building age. Second, we investigate how these parameters affect predictions of building downtime (i.e., reoccupancy time) as well as repair costs (i.e., building loss ratio). Although the physical dimensions of the building examined in Porter et al[11] are roughly equivalent to the 7-story building investigated in this study and the underlying seismic performance methodology examined is very similar, the type of sensitivity analysis conducted here is fundamentally different. Porter et al carried out a deterministic sensitivity analysis,[14] which used tornado diagrams to demonstrate the effects of changing different input variables one-at-a-time (OAT) to various discrete values, while keeping all others constant in a baseline model. We instead adopt a well-established variance-based (probabilistic) approach,[15] which accounts for the whole input space and measures sensitivity for an uncertain input variable in terms of its contribution to the variance of the output. Variance-based sensitivity analysis offers a more comprehensive understanding of the input–output interaction within a probabilistic seismic performance evaluation than the deterministic approach used by Porter et al, which is discussed in more detail in a later section.

We primarily examine high-level input parameters (hyperparameters) in this study (i.e., building age, building occupancy, lateral system, and ground shaking intensity), which provide basic information about the building and earthquake loading. These parameters influence the values of detailed parameters used within the P-58 analysis. For example, the building occupancy hyperparameter affects the types and quantities of nonstructural components populated in a P-58 building model, and the building age hyperparameter affects the vulnerability of the components. We focus mainly on the hyperparameters, as we assume that they are the dominant source of uncertainty (rather than the conditional detailed parameters) in most cases. However, we do consider some key detailed parameters that may have a significant impact on the model output (i.e., building period, which is dependent on the lateral system, and nonstructural component quantities, which are dependent on the building occupancy). Note that the FEMA P-58 methodology is not explicitly designed to handle uncertainty in many of the input variables investigated (i.e., lateral system, period, occupancy, age, and nonstructural component quantities). However, it is pertinent to treat these variables as uncertain in this case (and thus gain a proper understanding of their importance in the calculations), given that the level of effort required to precisely refine these inputs for the calculations can prove impractical for practitioners wishing to implement the methodology.[16]

This paper is structured as follows. In Section 2, we describe the variance-based sensitivity analysis procedure in the context of the FEMA P-58 methodology. In Section 3, we introduce the two case study buildings, and use them to calculate

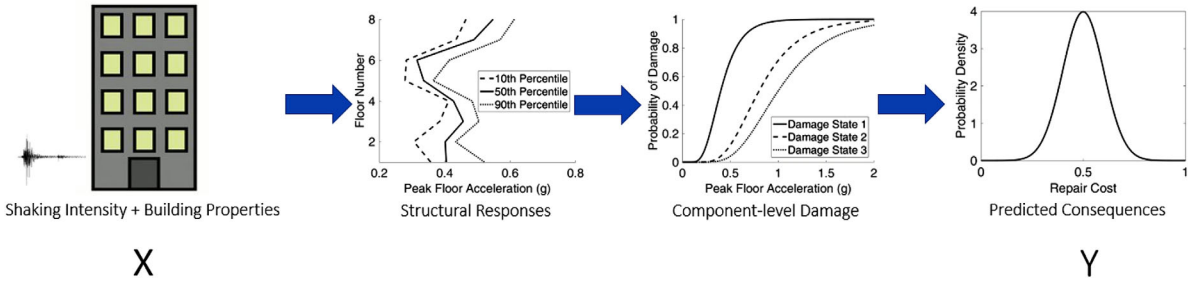

FIGURE 1 An overview of the FEMA P-58 methodology

Note. Model inputs ($\mathbf{X}$) consist of a description of the earthquake shaking intensity and building properties. Model outputs (Y) are consequence predictions in the form of repair costs, repair times, and casualties.

the variance-based sensitivity of P-58 repair cost and repair time predictions to different input parameters. In Section 4, we benchmark the Section 3 sensitivity analyses results using HAZUS. In Section 5, we describe the advantages of using the variance-based sensitivity analysis procedure over the deterministic sensitivity analysis procedure used by Porter et al In Section 6, we quantify the additional uncertainty in P-58 repair cost predictions that results from different input parameters being unknown, using one of the case study buildings.

2 | VARIANCE-BASED SENSITIVITY ANALYSES

We conduct variance-based sensitivity analyses in this study. For a given model of the form $Y = g(\mathbf{X})$, variance-based methods are probabilistic sensitivity analyses that quantify the sensitivity of Y to $\mathbf{X}$ in terms of a reduction in the variance of Y.[17] The function $g(\cdot)$ of interest in this study is the FEMA P-58 methodology.[12] Model inputs ($\mathbf{X}$) consist of a building's properties (such as lateral system, occupancy type, and age) and the shaking intensity at the building for a given level of earthquake loading. These inputs are used to generate Monte Carlo samples of the building's response, which in turn are input to component-level fragility functions to simulate damage. Finally, damage predictions are translated to consequences (Y), in the form of repair costs, repair times, and casualties. An overview of the methodology is presented in Figure 1.

The variance of Y across the whole input space ($V_{\mathbf{X}}[Y]$) can be decomposed as follows[18]:

$$V_{\mathbf{X}}[Y] = \sum_{i=1}^{p} V_i + \sum_{1 \le i < j \le p} V_{ij} + \cdots + V_{1\ldots p}, \tag{1}$$

where p is the number of input parameters. V_i measures the main effect of input parameter X_i on Y and is defined as follows[19]:

$$V_i = V_{X_i}[E_{\mathbf{X}_{\sim i}}(Y|X_i)], \tag{2}$$

where $V[\cdot]$ denotes variance, $E(\cdot)$ denotes expectation, and $\mathbf{X}_{\sim i}$ includes all inputs but X_i. In words, V_i is the expected reduction in variance that would be obtained if X_i could be fixed. The inner expectation operator takes the mean of Y over all possible values of $\mathbf{X}_{\sim i}$, for a fixed value of X_i. The outer variance is then taken over all possible values of X_i. The sensitivity measure associated with V_i is the first-order (main effect) sensitivity coefficient, defined as

$$S_i = \frac{V_{X_i}[E_{\mathbf{X}_{\sim i}}(Y|X_i)]}{V_{\mathbf{X}}[Y]}. \tag{3}$$

For example, an S_i value of 0.2 implies that fixing the value of X_i would reduce the variance of Y by 20% on average. V_{ij} measures the effect of the interaction between X_i and X_j on Y, i.e., it is the portion of variance in Y due to X_i and X_j that is not captured in the individual main effects of X_i and X_j:

$$V_{ij} = V_{X_iX_j}[E_{\mathbf{X}_{\sim ij}}(Y|X_i, X_j)] - V_{X_i}[E_{\mathbf{X}_{\sim i}}(Y|X_i)] - V_{X_j}[E_{\mathbf{X}_{\sim j}}(Y|X_j)]. \tag{4}$$

The total effect sensitivity index is another sensitivity measure that captures the effect of these (and higher order) interactions, in addition to the main effects. It therefore measures the total contribution of all terms in the variance decomposition that contain X_i. It is defined as

$$S_{Ti} = \frac{E_{\mathbf{X}_{\sim i}}(V_{X_i}[Y|\mathbf{X}_{\sim i}])}{V_{\mathbf{X}}[Y]}, \tag{5}$$

where $E_{\mathbf{X}_{\sim i}}(V_{X_i}[Y|\mathbf{X}_{\sim i}])$ is the expected variance that would remain if all inputs but X_i could be fixed, and $V_{\mathbf{X}}[Y]$ is as defined in Equation (1). We use the first-order sensitivity coefficient (Equation 3) as the metric of sensitivity in this study. The total effect sensitivity index (Equation 5) is used in the subsequent uncertainty quantification.

When inputs are correlated, they are grouped together as a multidimensional variable $\mathbf{X}_r$.[20] The first-order sensitivity coefficient becomes

$$S_r = \frac{V_{\mathbf{X}_r}[E_{\mathbf{X}_{\sim r}}(Y|\mathbf{X}_r)]}{V_{\mathbf{X}}[Y]}, \tag{6}$$

and the total effect sensitivity index is

$$S_{Tr} = \frac{E_{\mathbf{X}_{\sim r}}(V_{\mathbf{X}_r}[Y|\mathbf{X}_{\sim r}])}{V_{\mathbf{X}}[Y]}. \tag{7}$$

3 | CASE STUDIES

We investigate the sensitivity of Y to $\mathbf{X}$ for a 7-story and a 14-story building at an example site in downtown Los Angeles. The site is located at 34.0407°N, 118.2468°W. The 7-story building is 91 ft tall and 67,000 ft^2, while the 14-story building is 182 ft tall and 134,000 ft^2. Both buildings are assumed to be square in plan. We use the SP3 software tool[21] to run the FEMA P-58 analyses. The tool's calculated replacement value ranges from \$11,390,000 for a retail building to \$37,185,000 for a healthcare building in the case of the 7-story building, and it ranges from \$22,780,000 (retail) to \$74,370,000 (healthcare) for the 14-story building. We generate structural responses with the seismic response prediction engine[22] feature of the tool. This engine estimates responses based on observations from a large database of nonlinear structural models. A full list of the inputs provided to the engine can be found in Supporting Information Appendix A.

3.1 | Input variables (X)

The input variables ($\mathbf{X}$) investigated for the case study buildings are shaking intensity (X_1), lateral system (X_2), period (X_3), occupancy (X_4), age (X_5), and nonstructural component quantities (X_6). (These variables are fully defined in subsequent sections.) X_2, X_4, and X_5 are discrete variables with b possible values, which are assumed to follow a discrete uniform distribution in our analyses, i.e.,

$$F_{X_i}(x_i; b) = \frac{\lfloor x_i \rfloor}{b}, \tag{8}$$

where X_i is the discrete variable of interest, $\lfloor x_i \rfloor$ is the greatest integer less than or equal to x_i, and $F_{X_i}(x_i; b)$ is the CDF for $x_i \in [1, b]$. A uniform distribution is assumed for these variables, as it is the maximum entropy estimate. This approach enables us to draw very general conclusions about the importance of these parameters in the seismic loss calculations. However, it should be noted that maximum entropy is a conservative description of uncertainty, which may underestimate the level of knowledge available on these variables in real-life situations. For example, a simple visual examination of a building could significantly reduce its number of potential lateral systems and alter their relative probability. We therefore also provide additional sensitivity analyses results for cases where more specific information is known about these variables (in Supporting Information Appendix B). All other input variables are continuous, and their corresponding probability distributions are discussed in the following sections.

TABLE 1 Inputs provided to OpenSHA for obtaining the hazard curves (note that the use of more recent IMR and ERF parameters and/or inclusion of background seismicity do not have a significant effect on the curves obtained)

Parameter	Value
Intensity measure relationship	USGS combined (2004)
Gaussian truncation	No
Component	Average horizontal
Standard deviation type	Total
V_{S30} [m/s]	259
Earthquake rupture forecast (ERF)	USGS/CGS 2002 adjusted California
Fault model	Frankel's
Rupture offset [km]	10
Background seismicity	Exclude

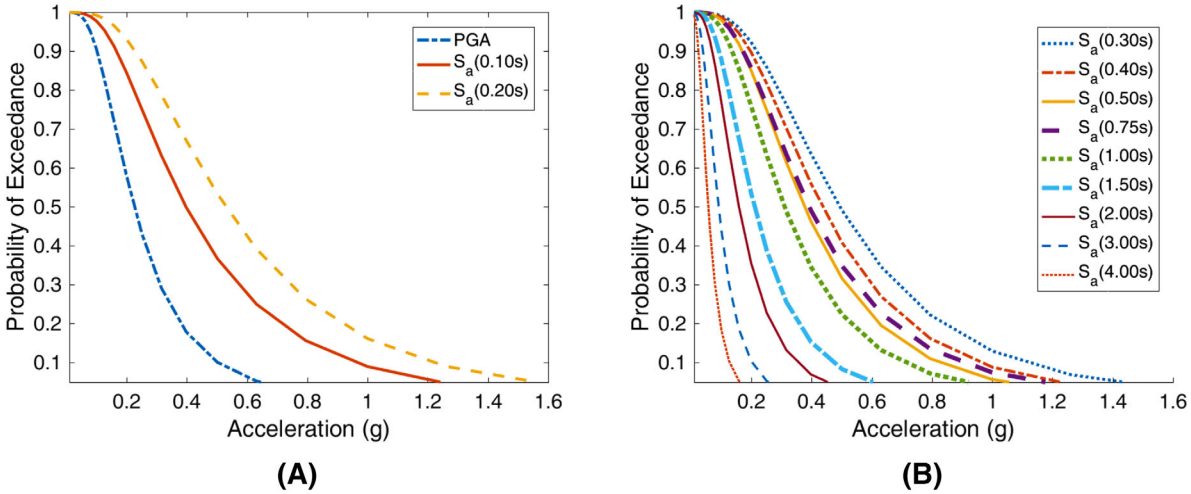

FIGURE 2 Fifty-year hazard curves at the case study site for spectral acceleration with 5% critical damping [$S_a(T)$], at the (A) short periods and (B) long periods provided in OpenSHA

3.1.1 | Shaking intensity

Peak ground acceleration (PGA) and spectral acceleration with 5% critical damping at the building's first-mode period [$S_a(T_1)$] are used to represent shaking intensity. Shaking intensity measures the severity of earthquake loading on the building, and therefore affects the building's response. It is taken from 50-year hazard curves at the site of interest, obtained in OpenSHA[23] using the inputs in Table 1. A 50-year duration is used because many authors assume a 50-year useful life of new construction.[24] The hazard curves are shown in Figure 2, at the periods provided in OpenSHA. We use shaking intensities with probabilities of exceedance between 5% and 95%. It is important to note that inclusion of exceedance probabilities further in the tails may modify the outcome of the sensitivity calculations. However, such values are neglected in this study due to the very rare occurrence of the corresponding shaking intensity. Exceedance values within this range are assumed to be uniformly distributed in our analyses (i.e., the maximum entropy estimate). We linearly interpolate between periods and acceleration values to obtain appropriate values of S_a for a given building period, using results obtained for available $S_a(T)$ periods.

Let X_1 represent shaking intensity probability of exceedance. The cumulative distribution function (CDF) for X_1 can be expressed as follows:

$$F_{X_1}(x_1) = \frac{x_1 - a_1}{b_1 - a_1}, \tag{9}$$

where $F(\cdot)$ denotes the CDF. $a_1 = 0.05$ and $b_1 = 0.95$ in this case.

TABLE 2 Median building periods ($\hat{T}$) assumed for each lateral system and both building sizes

Lateral system	$\hat{T}$ (s)	
	7-Story building	14-Story building
Concrete moment frame (perimeter)	1.03	1.91
Concrete moment frame (space)	1.03	1.91
Concrete shear wall	0.73	1.23
Steel eccentrically braced frame	1.11	1.86
Steel concentrically braced frame	1.11	1.86
Steel moment frame (perimeter)	1.36	2.36
Steel moment frame (space)	1.36	2.36
Steel moment frame and concrete shear wall	0.84	1.40

3.1.2 | Lateral system

This variable affects the type of structural components populated in each building model, as well as the building's response to a given level of ground shaking. We examine eight lateral systems in our analyses: (1) perimeter concrete moment frame, (2) space concrete moment frame, (3) concrete shear wall, (4) perimeter steel moment frame, (5) space steel moment frame, (6) steel eccentrically braced frame, (7) steel concentrically braced frame, and (8) steel moment frame and concrete shear wall. We use these lateral systems as they can be modeled in the seismic response prediction engine and estimates of their associated periods can be obtained from the HAZUS methodology.[25] The distribution of lateral system (X_2) is given by Equation (8) for $b = 8$.

3.1.3 | Period

This variable affects the building's response to a given level of ground shaking. The median building period in seconds ($\hat{T}$) is taken as the estimate obtained from HAZUS for the given lateral system and number of stories (see Table 2). We assume that period follows a lognormal distribution, which is consistent with the literature.[26–28] We assume that the logarithmic standard deviation of the period (β) is constant across all lateral systems and the two building heights studied. It is taken as 0.29, which is the square root of the average of the logarithmic variances of period (0.23^2, 0.209^2, 0.391^2) provided in Gilles et al[28] for steel moment resisting frame, reinforced concrete moment resisting frame, and reinforced concrete shear wall, respectively.

The CDF for building period (X_3) can be expressed as follows:

$$F_{X_3}(x_3) = \Phi\left(\frac{\ln(x_3/\hat{T})}{\beta}\right), \tag{10}$$

where $x_3 > 4$ is set to 4, to correspond with the maximum period for which the site's 50-year hazard curve is provided in OpenSHA (though $x_3 > 4$ values are rare). $F(\cdot)$ is the lognormal CDF, and $\Phi(\cdot)$ is the standard normal CDF. Note that X_3 is dependent on X_2, so the sensitivities of the two input variables are measured together according to Equations (6) and (7). The two input variables will collectively be referred to as "lateral system" in our analyses.

3.1.4 | Occupancy

This variable affects the types and quantities of nonstructural components populated in each building model. We examine 9 of the 10 occupancy types included in P-58 in our analyses: (1) office, (2) elementary school, (3) middle school, (4) high school, (5) healthcare, (6) hospitality, (7) research, (8) retail, and (9) multiunit residential. The warehouse occupancy type is not considered because we are looking at 7- and 14-story buildings. The distribution of occupancy (X_4) is given by Equation (8) for $b = 9$.

3.1.5 | Age

This variable affects the vulnerability of components populated in each building model. We investigate four different building design eras (ages) in this study: pre-1941, 1941–1976, 1976–1994, and post-1994. The boundaries of each era are chosen to coincide with years in which significant changes occurred to U.S. seismic design codes. Note that many nonstructural components used in the SP3 software correspond to a specific seismic design category (SDC), a concept that was only introduced in more recent seismic design codes.[29] SDC D is the correct design category for the two case studies, given the site location. We use nonstructural components with other values of SDC for pre-1994 buildings, to account for the less stringent seismic design provisions in effect at those times. Each SDC has an associated range of short period spectral acceleration (S_{DS}) values, which are used to calculate the capacity of anchored nonstructural components. We use the middle value of the corresponding range for pre-1994 buildings, and the site-specific value calculated according to 2008 USGS hazard maps[30] (assuming site class D) for post-1994 buildings. Note that for pre-1976 buildings, mechanical components are assumed to be unanchored, and the S_{DS} value is only used to calculate the out-of-plane capacity of cladding. Full details of our assumptions for each building age are as follows:

1. Pre-1941: We assume that the building code is the 1935 uniform building code (UBC).[31] We use SDC A components and set $S_{DS} = 0.17g$. We assume that mechanical components are not anchored, elevators were those typically installed in California prior to 1976, stairs do not have seismic joints, and pendant lighting is nonseismic.
2. 1941–1976: We assume that the building code is the 1955 UBC.[32] We use SDC B components and set $S_{DS} = 0.33g$. We assume that mechanical components are not anchored, elevators were those typically installed in California prior to 1976, stairs do not have seismic joints, and pendant lighting is nonseismic.
3. 1976–1994: We assume that the building code is the 1976 UBC.[33] We use SDC C components (SDC D for healthcare) and set $S_{DS} = 0.50g$ ($S_{DS} = 1.56g$ for healthcare nonstructural components). We assume that mechanical components are vibration isolated (hard anchored for healthcare), stairs have seismic joints, elevators were those typically installed in California post-1976, and pendant lighting is seismically rated.
4. Post-1994: We assume that the building code is ASCE 7-10.[34] We use SDC D components and set $S_{DS} = 1.56g$. We assume that mechanical components are hard anchored, stairs have seismic joints, elevators were those typically installed in California post-1976, and pendant lighting is seismically rated.

The distribution of age (X_5) is given by Equation (8) for $b = 4$.

3.1.6 | Nonstructural component quantities

This parameter affects the quantities of nonstructural components populated in each building model, given the value of the occupancy variable (X_4). We include it in our analyses because nonstructural components are the primary source of earthquake-induced loss in most buildings,[35] and their quantity may have a notable impact on the model outputs. We assume that the quantities follow the lognormal distributions for each component provided in the P-58 Normative Quantity Estimation Tool.[36] The parameters of the lognormal distributions depend on the value of X_4. We assume that quantities of the same component are identical on different floors, and that there is perfect correlation between quantities of all nonstructural components, which implies that the percentile of the sampled quantity is identical for all nonstructural components in a given P-58 Monte Carlo sample.

Let X_6 denote nonstructural component quantity percentile. We assume that X_6 follows a uniform distribution in our analysis, therefore the CDF of X_6 is

$$F_{X_6}(x_6) = \frac{x_6 - a_6}{b_6 - a_6}, \tag{11}$$

where $F(\cdot)$ denotes the CDF. $a_6 = 0$ and $b_6 = 100$ in this case. The corresponding quantity of a given nonstructural component is then obtained using the appropriate lognormal distribution parameters as follows:

$$q = G^{-1}\left(\frac{x_6}{100}\right) = \ln(\hat{q}) + \beta_q \Phi^{-1}\left(\frac{x_6}{100}\right), \tag{12}$$

where q is the quantity of the nonstructural component of interest, $G^{-1}(\cdot)$ is the inverse CDF of the lognormal distribution, $\Phi^{-1}(\cdot)$ is the inverse standard normal CDF, $\hat{q}$ is the median quantity of the component and β_q is the logarithmic standard deviation of the quantity. $\hat{q}$ and β_q are obtained directly from the P-58 Normative Quantity Estimation Tool, for the given value of X_4.

Note that the procedure is slightly different for cladding and glazing because the combined quantity of these two components must cover the exterior building area. We assume that x_6% of the exterior building area is covered in cladding, and the rest is covered in glazing.

3.2 | Output variables (Y)

The output variables (Y) investigated for the case study buildings are building loss ratio (Y_{LR}) and reoccupancy time (Y_{RT}).

3.2.1 | Building loss ratio

This is the total repair cost of the building as a fraction of the replacement value. It is computed as follows:

$$Y_{LR}^{(j)} = LR^{(j)} = \frac{\sum_i^m RC_i^{(j)}}{ReplC}, \tag{13}$$

where $LR^{(j)}$ is the building loss ratio for the jth Monte Carlo sample, $RC_i^{(j)}$ is the repair cost of the ith component in the building for the jth Monte Carlo sample, $ReplC$ is the replacement cost of the building, and m is the total number of components in the building. Note that the replacement value of the building for a given building area varies as a function of the occupancy input variable.

3.2.2 | Reoccupancy time

Reoccupancy time is computed using the REDi rating system,[37] which was developed to aid stakeholders in resilience-based design. Reoccupancy time (RT) is defined in REDi as the time when the building is deemed safe enough to be used for shelter, and is the first recovery state of a building after an earthquake. It is a combination of delays due to impeding factors (IF) and the time required to repair heavily damaged structural and nonstructural components that pose a life-safety risk ($RepT$), i.e.,

$$Y_{RT}^{(j)} = RT^{(j)} = IF^{(j)} + RepT^{(j)} \tag{14}$$

for the jth Monte Carlo sample. Impeding factors are circumstances that prevent the initiation of building repairs: postearthquake inspection, engineering mobilization and review/redesign, financing, contractor mobilization and bidding, permitting, and procurement of components with long lead-time. Both impeding factors and component repairs are organized into logical sequences.[37] Worker allocations for component repairs are summarized in Table 3. These are obtained from Almufti and Willford[37] using Tables 6 and 7 as well as the equation on page 84 of the document.

3.3 | Calculating sensitivity indices

We generate 2000 Monte Carlo samples of each of the six inputs, according to the corresponding probability distributions summarized in Equations (8)–(12). We use a Latin hypercube sampling (LHS) design, which has been shown to produce more efficient sensitivity estimates than simple random sampling.[38] The 2000×6 Monte Carlo samples are used to construct matrix $\mathbf{A}$, termed as the "sampling matrix":

TABLE 3 Worker allocations for component repairs

	7-Story building	14-Story building
Workers per repair sequence		
Structure	0.002 Workers/ft^2	
Interior	0.001 Workers/ft^2	
Exterior	0.001 Workers/ft^2	
Mechanical	3 Workers/damaged component	
Electrical	3 Workers/damaged component	
Elevator	2 Workers/damaged component	
Stairs	2 Workers/damaged component	
Maximum workers		
Interior	27	30
Exterior	27	30
Mechanical		18
Electrical		18
Elevator		12
Stairs		12
On site	27	44

$$\mathbf{A} = \begin{bmatrix} x_1^{(1)} & x_2^{(1)} & \dots & x_6^{(1)} \\ x_1^{(2)} & x_2^{(2)} & \dots & x_6^{(2)} \\ \vdots & \vdots & \ddots & \vdots \\ x_1^{(2000)} & x_2^{(2000)} & \dots & x_6^{(2000)} \end{bmatrix}. \tag{15}$$

Note that $x_1, x_2, \dots, x_6$ are as defined in Sections 3.1.1–3.1.6. We generate a further 2000 Monte Carlo samples of each of the input variables using LHS, independent of matrix **A**. These Monte Carlo samples are used to construct matrix **B**, termed as the "resampling matrix":

$$\mathbf{B} = \begin{bmatrix} x_1^{(2001)} & x_2^{(2001)} & \dots & x_6^{(2001)} \\ x_1^{(2002)} & x_2^{(2002)} & \dots & x_6^{(2002)} \\ \vdots & \vdots & \ddots & \vdots \\ x_1^{(4000)} & x_2^{(4000)} & \dots & x_6^{(4000)} \end{bmatrix}. \tag{16}$$

We construct the third sampling matrix $\mathbf{C}_i$ by substituting the ith column of matrix **A** for the ith column of matrix **B**:

$$\mathbf{C}_i = \begin{bmatrix} x_1^{(2001)} & \dots & x_i^{(1)} & \dots & x_6^{(2001)} \\ x_1^{(2002)} & \dots & x_i^{(2)} & \dots & x_6^{(2002)} \\ \vdots & \ddots & \vdots & \ddots & \vdots \\ x_1^{(4000)} & \dots & x_i^{(2000)} & \dots & x_6^{(4000)} \end{bmatrix}. \tag{17}$$

We then construct the final sampling matrix $\mathbf{D}_i$ by substituting the ith column of matrix **B** for the ith column of matrix **A**:

$$\mathbf{D}_i = \begin{bmatrix} x_1^{(1)} & \dots & x_i^{(2001)} & \dots & x_6^{(1)} \\ x_1^{(2)} & \dots & x_i^{(2002)} & \dots & x_6^{(2)} \\ \vdots & \ddots & \vdots & \ddots & \vdots \\ x_1^{(2000)} & \dots & x_i^{(4000)} & \dots & x_6^{(2000)} \end{bmatrix}. \tag{18}$$

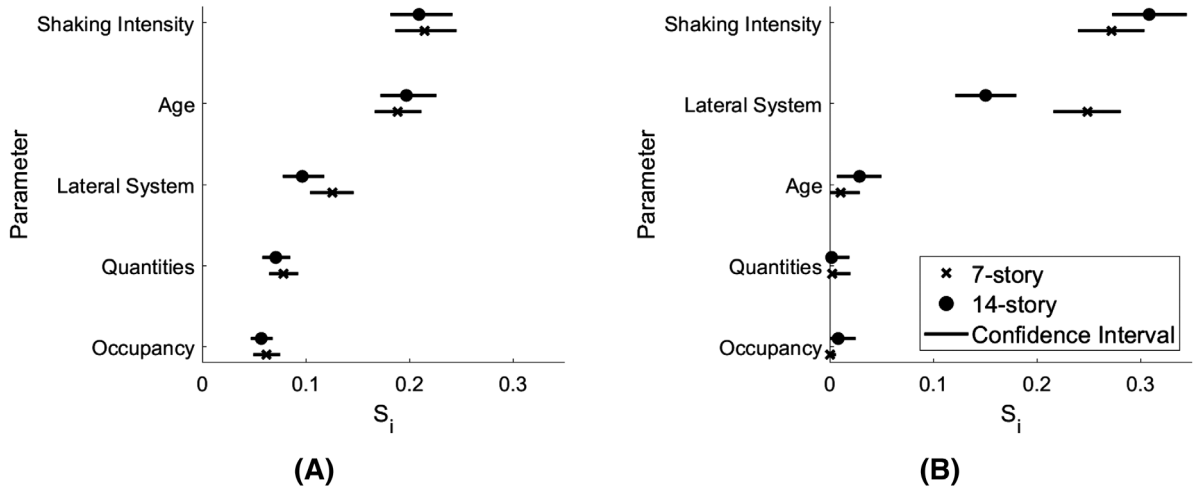

FIGURE 3 First-order sensitivity coefficients of input variables examined for (A) building loss ratio and (B) reoccupancy time

As lateral system (X_2) and building period (X_3) are correlated inputs in our study, there is only one set of input matrices generated for both variables. The corresponding $\mathbf{C}_r$ matrix is obtained by substituting both the second and third columns of matrix $\mathbf{A}$ for the second and third columns of matrix $\mathbf{B}$. The corresponding $\mathbf{D}_r$ matrix is obtainedanalogously.

$\mathbf{A}$, $\mathbf{B}$, $\mathbf{C}_i$, and $\mathbf{D}_i$ are each used in a separate FEMA P-58 analysis, and each row of the given input matrix provides the values of the input variables for one P-58 Monte Carlo simulation. The output variables obtained using each input matrix (Y_A, Y_B, Y_{C_i}, and Y_{D_i}) are then used to estimate the sensitivity indices presented in Section 2. The first-order sensitivity coefficient (defined in Equation 3) is estimated as[19]

$$S_i = \frac{(1/2N)(\sum_{j=1}^{N} Y_A^{(j)} Y_{C_i}^{(j)} + \sum_{j=1}^{N} Y_B^{(j)} Y_{D_i}^{(j)}) - \hat{f}_0^2}{(1/2N)\sum_{j=1}^{N}[(Y_A^{(j)})^2 + (Y_B^{(j)})^2] - \hat{f}_0^2} \tag{19}$$

and the total effect sensitivity index (defined in Equation 5) is estimated as[19]

$$S_{Ti} = 1 - \frac{(1/2N)(\sum_{j=1}^{N} Y_B^{(j)} Y_{C_i}^{(j)} + \sum_{j=1}^{N} Y_A^{(j)} Y_{D_i}^{(j)}) - \hat{f}_0^2}{(1/2N)\sum_{j=1}^{N}[(Y_A^{(j)})^2 + (Y_B^{(j)})^2] - \hat{f}_0^2}, \tag{20}$$

where $\hat{f}_0^2 = \frac{1}{2N}\sum_{j=1}^{N}(Y_A^{(j)} Y_B^{(j)} + Y_{C_i}^{(j)} Y_{D_i}^{(j)})$ from Yun et al[39] These estimates are derived using the well-known identity $V[Z] = E(Z^2) - E^2(Z)$.

3.4 | Sensitivity analyses results

Values of S_i are presented in Figure 3 for both case study buildings and both FEMA P-58 consequence predictions of interest. A total of 10,000 bootstrap samples were used to account for uncertainty in S_i per Archer et al,[40] with the confidence bounds taken as the 2.5th and 97.5th percentiles of the bootstrapped samples. Results of the sensitivity analyses are very similar for both buildings, indicating that the height of the building does not significantly affect the sensitivities of the loss predictions. It can be seen that shaking intensity and age are the most important input variables for predicting building loss ratio, while shaking intensity and lateral system are most important for predicting reoccupancy time. It is interesting to note that reoccupancy time is significantly less sensitive to age than building loss ratio. This may be explained by the fact that there is generally larger uncertainty in damage-to-loss functions for repair time than repair cost (and therefore a reduced relative contribution of the age input variable to the overall variance of the output). In addition, mean repair cost differences tend to be significantly larger than mean repair time differences across different damage states of a given component.

The values of S_i obtained may seem counterintuitively low, but they make sense if we consider the composition of $V_{\mathbf{X}}[Y]$ (i.e., the denominator of S_i) in Equation (3). This variable accounts for variance across the whole input space, including that of many input variables not being explicitly examined in this study (e.g., engineering demand parameters conditioned on the chosen hyperparameters, damage conditioned on the engineering demand parameters, etc.), as well as the combined effect of uncertain variables. S_i values on the order of 0.1 or 0.2 should therefore be considered notable.

Supporting Information Appendix B contains additional sensitivity analyses results for the 7-story case study building, when different levels of information are known about lateral system and occupancy. It can be seen that the conclusions of the sensitivity analyses can change, depending on the information known. For example, the sensitivity of building loss ratio to lateral system is significantly lower if the building is known to be made of concrete (Figure 10 in Supporting Information Appendix B).

4 | BENCHMARKING SENSITIVITY ANALYSIS RESULTS USING HAZUS

We conduct further variance-based sensitivity analyses using the HAZUS earthquake loss estimation methodology[25] for the same case study buildings, to investigate if the impacts of different input variables on the outputs are similar to those observed with P-58. The input matrix $\mathbf{X}$ for HAZUS consists of shaking intensity (in the form of PGA), lateral system, age, and occupancy. These inputs are used to compute structural and nonstructural loss ratios, via building-level fragility functions. Note that we use equivalent PGA fragility functions in this study, which are outlined in Section 5.4.4 of.[25] The model output Y is an aggregation of the structural and nonstructural loss ratios. This is equivalent to the building loss ratio output of the FEMA P-58 methodology.

The lateral system, occupancy, and age input variables used for FEMA P-58 need to be adjusted for use in HAZUS. A summary of the necessary adjustments is provided in Table 4. Mid-rise HAZUS fragility functions are used for the 7-story building, and high-rise fragility functions are used for the 14-story building. The nonstructural component quantities input variable is not used because it is not considered in the HAZUS methodology. HAZUS analyses are also conducted using 2000 Monte Carlo simulations of the input variables. To be consistent with the FEMA P-58 methodology, we deviate slightly from[25] and sample damage states from the building fragility functions for each Monte Carlo simulation, instead of using mean damage states. The building loss ratio is then calculated based on the sampled damage state.

Figure 4 compares the S_i values obtained using FEMA P-58 and HAZUS for building loss ratio. It is clear that the general trend in S_i across the different input variables is approximately the same for the two procedures, and similar values of S_i are obtained using both procedures in most cases. There is a notable difference in the 7-story building S_i value for lateral system, but this is not unexpected given that the number of potential values of lateral system is eight in FEMA P-58 and only five in HAZUS (see Table 4).

Figure 5 compares P-58 and HAZUS building loss ratio predictions for the 14-story building, as a function of each input variable examined. Note that shaking intensity is expressed in terms of PGA, the shaking intensity input of the HAZUS methodology. All input variables except that plotted on the x-axis are kept constant for each plot. Constant values of each input variable are PGA (and $S_a(T_1)$ for FEMA P-58) with 50% probability of exceedance for shaking intensity, 1976–1994 (moderate code) for age, concrete shear wall for lateral system, office for occupancy, and median nonstructural component quantities (only for FEMA P-58). It can be seen that the trend in building loss ratio across PGA is almost identical for both methodologies, which makes sense given the similar values of S_i obtained for shaking intensity using both methods. The range in mean building loss ratio values obtained across the different values of lateral system, age, and occupancy is larger for P-58 than HAZUS, which is consistent with the difference in S_i values observed for these variables.

5 | ADVANTAGES OF VARIANCE-BASED SENSITIVITY ANALYSES

For probabilistic methodologies such as P-58, the variance-based approach adopted in this work has a number of benefits over the OAT deterministic analyses used in a similar previous study by Porter et al,[11] such that it provides better insight into the interactions between the inputs and outputs of the procedure. For example, variance-based sensitivity analyses implicitly handle possible correlations in the input variables of interest. Correlations cannot be considered in OAT analyses[41] because this would require the simultaneous movement of more than one input variable.[42] This makes it difficult to identify appropriate sets of input variable values to use in deterministic analyses,[43] and may result in substantial biases.[44] The whole input space is accounted for in variance-based sensitivity analyses, whereas only a

TABLE 4 Assumed mapping from FEMA P-58 lateral system, occupancy, and age input variables to corresponding HAZUS classes

FEMA P-58	HAZUS
Lateral system	
Concrete moment frame (perimeter)	Concrete moment frame (C1)
Concrete moment frame (space)	Concrete moment frame (C1)
Concrete shear wall	Concrete shear wall (C2)
Steel eccentrically braced frame	Steel braced frame (S2)
Steel concentrically braced frame	Steel braced frame (S2)
Steel moment frame (perimeter)	Steel moment frame (S1)
Steel moment frame (space)	Steel moment frame (S1)
Steel moment frame and concrete shear wall	Steel frame, concrete shear walls (S4)
Occupancy	
Office	Professional/technical/business services (COM4)
Elementary school	Schools/libraries (EDU1)
Middle school	Schools/libraries (EDU1)
High school	Schools/libraries (EDU1)
Healthcare	Hospital (COM6)
Hospitality	Temporary lodging (RES4)
Research	Colleges/universities (EDU2)
Residential	Multi family dwelling (RES3)
Retail	Retail trade (COM1)
Age	
Pre-1941	Pre-code
1941–1976	Low code
1976–1994	Moderate code
Post-1994	High code

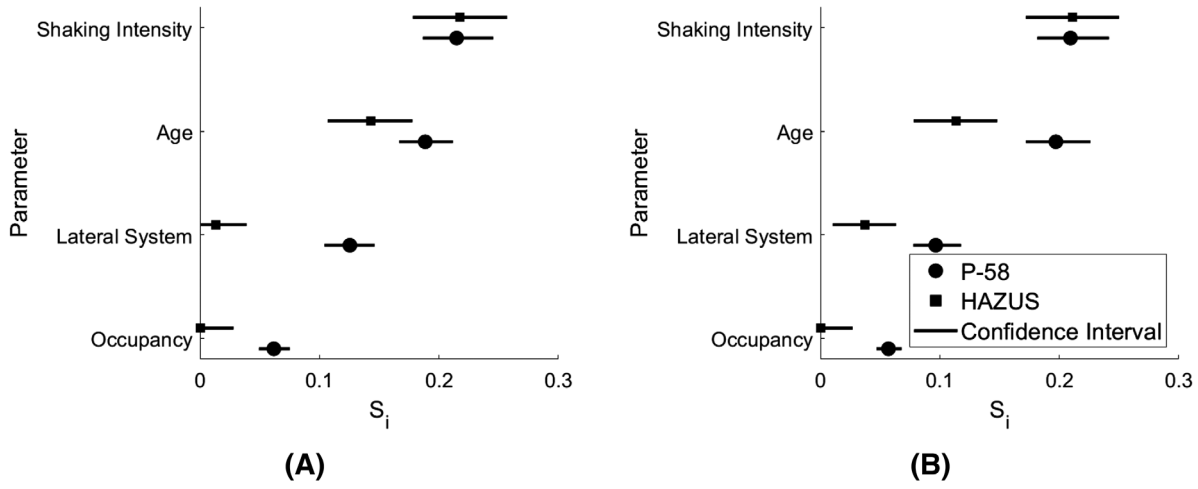

FIGURE 4 Benchmarking P-58 sensitivity indices against those of HAZUS for (A) the 7-story building and (B) the 14-story building

small proportion of this space is explored in OAT deterministic analyses[45]; although this makes the latter approach more computationally efficient, the associated range in values of the output may be too narrow.[17]

Here, we illustrate some of the limitations of OAT deterministic sensitivity analyses that do not arise in variance-based sensitivity analyses, using data examined in this study. We conduct an OAT deterministic sensitivity analysis for the 7-story building. The baseline model is a concrete shear wall elementary school of 1976–1994 design, with median building period,

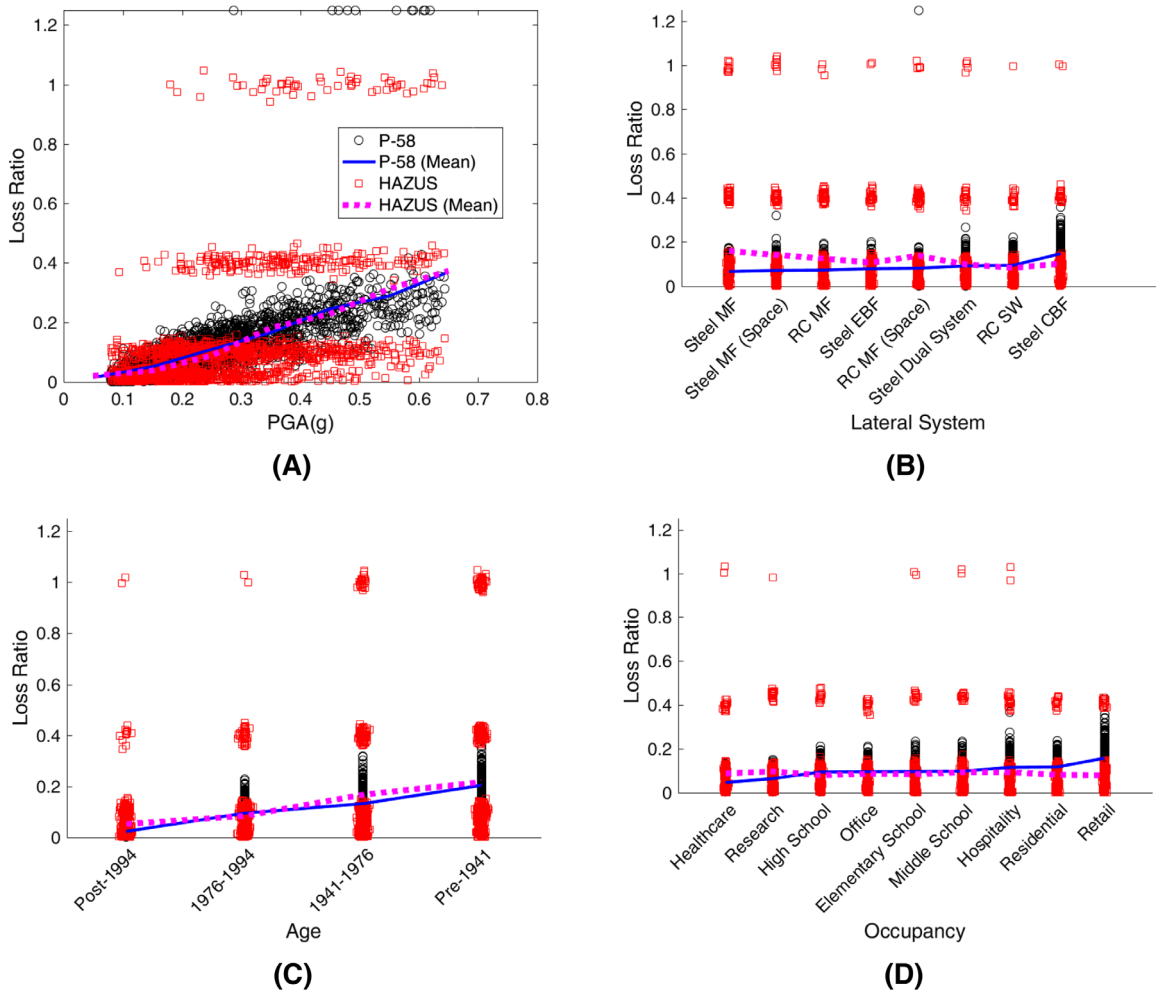

FIGURE 5 Comparison of P-58 and HAZUS building loss ratio predictions as a function of (A) shaking intensity (*PGA*), (B) lateral system, (C) age, and (D) occupancy

Note. Each symbol on a plot represents the prediction for one simulation of the P-58 or HAZUS methodology. P-58 building loss ratios greater than 1 indicate simulations in which the building collapsed, and account for the cost of demolition as well as building replacement. Simulations having identical values of HAZUS building loss ratio are offset vertically in all plots, and horizontally in (B)–(D), to aid visualization. The mean building loss ratio is a rolling average of predictions over 0.1*g*-wide bins of *PGA* in (A), and the mean of each value of the input variable in (B)–(D).

median nonstructural component quantities, and subjected to shaking intensity with 50% probability of exceedance. The extreme values of the three continuous variables are the 5th and 95th percentiles. We investigate the sensitivity of the building loss ratio to each input variable.

Figure 6A shows that the building loss ratio can appear more or less sensitive to nonstructural component quantities in the OAT deterministic sensitivity analysis, depending on the extreme values examined for the input parameter. The issue of choosing appropriate extreme values does not arise with variance-based sensitivity analysis because the whole input space is accounted for.

Figure 6B demonstrates that the OAT deterministic sensitivity analysis cannot handle correlation of the lateral system and period input variables. The importance of the lateral system variable changes, depending on the percentile of period used. Variance-based sensitivity analysis implicitly captures the correlation between lateral system and period, by sampling from the joint probability distribution of the input variables. Figure 6A,B demonstrates that variations in input parameter assumptions can create differences in the overall trend of the results for OAT deterministic sensitivity analysis, which may lead to misinformed decision-making on the prioritization of additional input data gathering.

Figure 6C highlights a further limitation of OAT deterministic sensitivity analysis. Let X_3^* denote an alternative version of the occupancy input variable, which follows a discrete uniform distribution with only four possible values: elementary

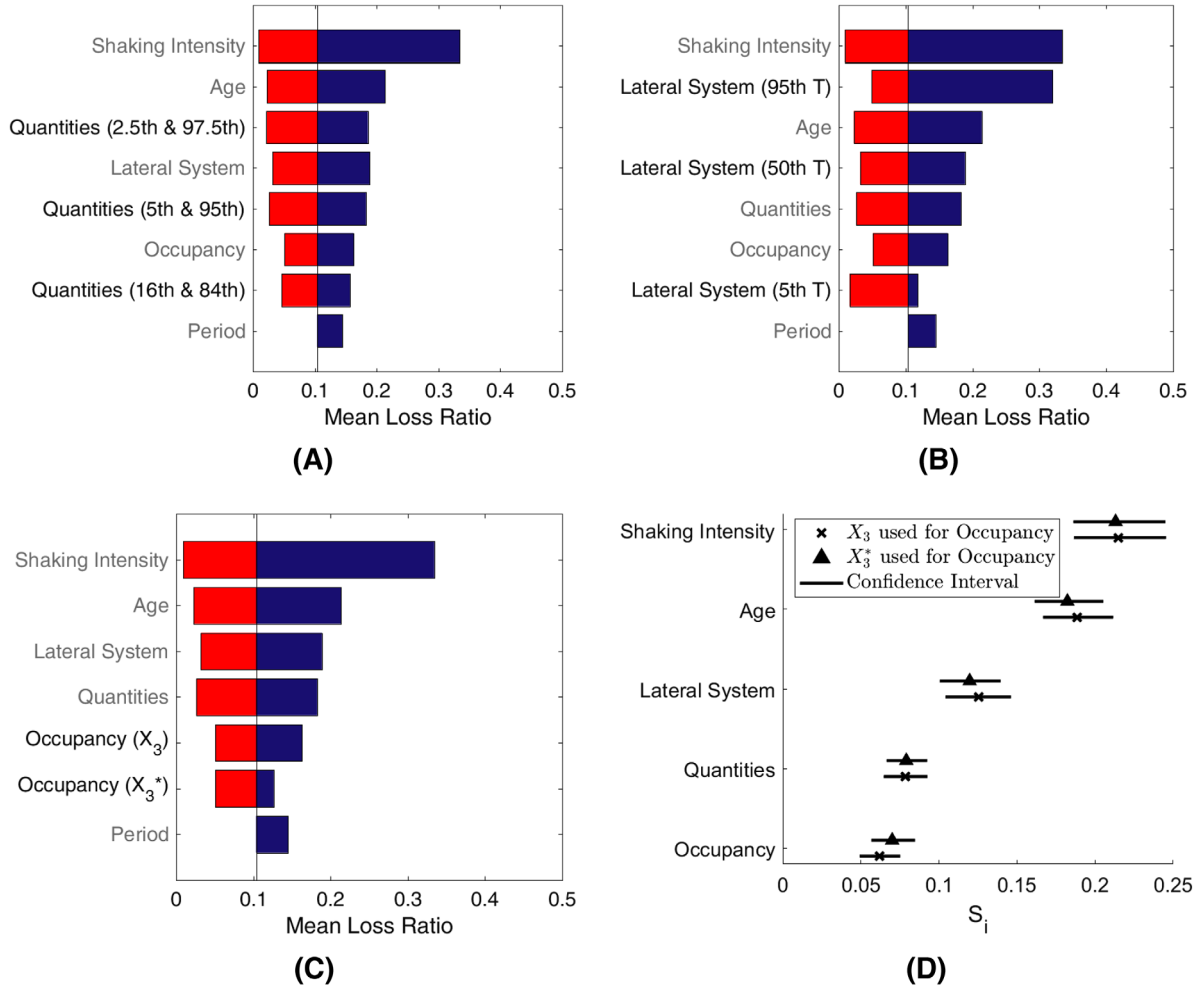

FIGURE 6 Deterministic sensitivity analysis results for the baseline model and (A) nonstructural component quantities with different extreme value percentiles (provided in parentheses); (B) lateral system, for different percentiles of period (T); (C) occupancy, when X_3^* is used instead of X_3. (D) variance-based sensitivity analyses results when X_3 and X_3^* are used for occupancy

school, healthcare, hospitality, and residential. The building loss ratio output obtained using $\mathbf{X}$ with X_3^* substituted for X_3 has the same mean and standard deviation as that obtained using the original $\mathbf{X}$. This is captured in variance-based sensitivity analyses, which produce almost identical first-order sensitivity coefficients when either X_3 or X_3^* is used in $\mathbf{X}$ (Figure 6D). However in OAT deterministic sensitivity analyses, the magnitude of the swing in occupancy is larger if all nine values are considered than if only the four values of X_3^* are considered. This incorrectly suggests that building loss ratio is less sensitive to the four values of X_3^* than the nine values of X_3.

6 | UNCERTAINTY QUANTIFICATION

The purpose of this section is to estimate the additional uncertainty in a P-58 model output that results when different model inputs are unknown. We then use the quantified uncertainty to estimate the adapted distribution of the model output for the unknown model inputs. It is important to note that results in this section are only obtained for the 14-story case study building, and may not be directly applicable to other building models. However, the general uncertainty quantification methodology presented is sufficiently flexible for application to any other case.

Let $Y_k = Y|\mathbf{X}$ denote a P-58 model output for a set of known (fixed) model inputs in $\mathbf{X}$. Figure 7 shows different Y_k (i.e., building loss ratio) of the 14-story case study building, for fixed values of shaking intensity, occupancy, age, and nonstructural component quantities (collectively denoted as $\mathbf{X}_{\sim 2}$), and each possible fixed value of lateral system (X_2). Let $Y_u = Y|\mathbf{X}_{\sim m}$ denote the adapted model output for the unknown model inputs $\mathbf{X}_m$. Y_u is demonstrated in Figure 7 for

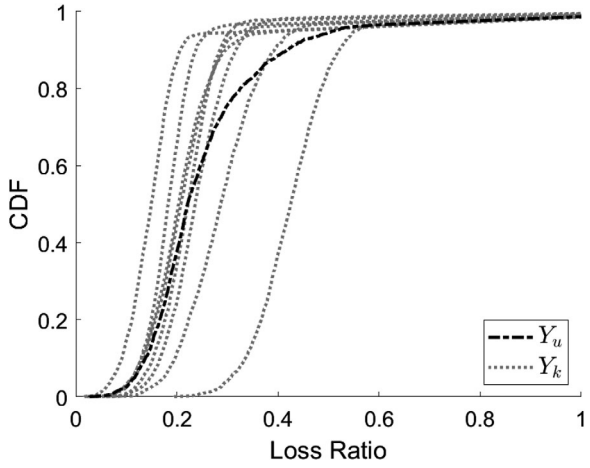

FIGURE 7 Empirical cumulative distribution functions (CDFs) of Y_k for all possible fixed values of lateral system (X_2) and fixed $\mathbf{X}_{\sim 2}$. Also shown is the empirical CDF of Y_u for unknown X_2 and fixed $\mathbf{X}_{\sim 2}$.

the fixed input variables $\mathbf{X}_{\sim 2}$ and unknown X_2. Note that we only consider the building loss ratio model output in this section, and we assume that shaking intensity will always be known.

We can quantify the expected increase in uncertainty of Y_k due to a given unknown model input X_i using a variance amplification metric (VA), defined as follows:

$$VA = E_{\mathbf{X}_{\sim i}}(V_{X_i}[Y|\mathbf{X}_{\sim i}]) - V[Y_k] = S_{Ti} \times V_{\mathbf{X}}[Y] - V[Y_k] = E(V[Y_u]) - V[Y_k], \tag{21}$$

where $E_{\mathbf{X}_{\sim i}}(V_{X_i}[Y|\mathbf{X}_{\sim i}])$ is the expected variance if all but X_i is fixed (from Equation 5), $V[Y_k]$ is the variance of Y_k, S_{Ti} is the total effect sensitivity index defined in Equation (5), $V_{\mathbf{X}}[Y]$ is the variance of the model output across the whole input space, and $E(V[Y_u])$ is the expected variance of $Y_u = Y|\mathbf{X}_{\sim i}$. A challenge with this formulation of VA is its dependence on Y_k, as this makes it specific to the corresponding set of fixed model inputs in $\mathbf{X}$. We propose an adapted version of the metric, $\hat{VA}$, that can be used to quantify the variance amplification for any Y_k. It is defined as follows:

$$\hat{VA} = S_{Ti} \times V_{\mathbf{X}}[Y] - V\left(Y_k^*\right) = E\left(V\left[Y_u\right]\right) - V\left[Y_k^*\right], \tag{22}$$

where S_{Ti} and $V_{\mathbf{X}}[Y]$ are as defined in Equation (21), and $V[Y_k^*]$ is the variance of Y_k^*. Y_k^* is a specified instance of Y_k that depends on X_i. We find Y_k^* for unknown X_i using the following steps:

1. We set all known variables except shaking intensity (X_1) to their median values ($\tilde{\mathbf{X}}_{\sim 1,i}$). The median values of input variables are those that produce $\tilde{Y}_k \approx \tilde{Y}_{\mathbf{X}}$ for shaking intensity with 50% probability of exceedance. ($\tilde{\cdot}$) is the median, $Y_{\mathbf{X}}$ is the model output considering the whole input space, and Y_k is as defined in Equation (21).
2. We use $\tilde{\mathbf{X}}_{\sim 1,i}$ with randomly sampled values of X_i to produce Y_u for shaking intensity at different points on the hazard curve. We investigate 10–90% probability of exceedance values for shaking intensity in intervals of 5%.
3. We find Y_u for which $V[Y_u] \approx E(V[Y_u]) = S_{Ti} \times V_{\mathbf{X}}[Y]$. $Y_k^* = Y_k$ for this value of shaking intensity, $\tilde{\mathbf{X}}_{\sim 1,i}$, and X_i set to its median value.

Table 5 provides values of $\hat{VA}$ and the corresponding standard deviation ($\sqrt{\hat{VA}}$), for each unknown input variable. Note that the shaking intensity for Y_k^* is the 25% probability of exceedance value in all cases. $\hat{VA}$ is largest for age, and there is no variance amplification for either unknown occupancy or nonstructural component quantities. These observations are in line with the results of the sensitivity analyses in Section 3.4.

For a given set of input variables $\mathbf{X}_{\sim i}$ with fixed values and unknown input variable X_i, we define $\hat{Y}_k = Y_k$ for the fixed values of $\mathbf{X}_{\sim i}$ and X_i set to its median value. We can use $\hat{VA}$ to predict the standard deviation of Y_u ($\hat{\sigma}_{Y_u}^{Amp}$), using the following equation:

TABLE 5 Uncertainty quantification for unknown input variables

Unknown input variable	Median value	S_{Ti}	$\hat{V}A$	$\sqrt{\hat{V}A}$
Lateral system	Steel moment frame and concrete shear wall	0.38	0.001	0.04
Occupancy	Office	0.32	0	0
Age	1976–1994	0.50	0.004	0.07
Nonstructural quantities	50th percentile	0.33	0	0

$$\hat{\sigma}_{Y_u}^{Amp} = \sqrt{\hat{V}A + V[\hat{Y}_k]}. \tag{23}$$

We estimate Y_u with a lognormal distribution, assuming that the mean of Y_u ($\bar{Y}_u$) is equivalent to that of the corresponding $\hat{Y}_k$, and the standard deviation of Y_u is $\hat{\sigma}_{Y_u}^{Amp}$. Let $\hat{Y}_u^{Amp}$ denote our estimate of Y_u. The parameters of $\ln \hat{Y}_u^{Amp}$ are calculated as follows:

$$\mu_{\ln \hat{Y}_u^{Amp}} = \ln\left(\bar{Y}_u^2 / \sqrt{\hat{\sigma}_{Y_u}^{Amp\,2} + \bar{Y}_u^2}\right) \tag{24}$$

$$\sigma_{\ln \hat{Y}_u^{Amp}} = \sqrt{\ln\left(\hat{\sigma}_{Y_u}^{Amp\,2} / \bar{Y}_u^2 + 1\right)}. \tag{25}$$

Figure 8 shows CDFs of $\hat{Y}_u^{Amp}$ for each unknown X_i and shaking intensity with 10% probability of exceedance. $\mathbf{X}_{\sim 1,i}$ are fixed at their median values ($\tilde{\mathbf{X}}_{\sim 1,i}$). The CDFs of $\hat{Y}_u^{Amp}$ are compared to empirical CDFs of observed Y_u. Also shown are Y_k for each possible value of unknown X_i (only 1st, 50th, and 99th percentile values are shown for nonstructural component quantities) and $\tilde{\mathbf{X}}_{\sim 1,i}$. $\hat{Y}_u^{Amp}$ appears to align well with the observed Y_u, for each unknown X_i. Equivalent figures for other values of shaking intensity (50%, 20%, and 6% probabilities of exceedance) can be found in Supporting Information Appendix C. $\hat{Y}_u^{Amp}$ appears to align well with the observed Y_u, for each unknown X_i at each of these levels of shaking intensity.

6.1 | Uncertainty quantification for pairs of unknown input variables

The uncertainty quantification method can also be used when pairs of input variables are unknown. $\hat{V}A$ is still calculated using Equation (22), except that S_{Ti} becomes S_{Tij}, defined as follows:

$$S_{Tij} = \frac{E_{\mathbf{X}_{\sim ij}}(V_{X_i X_j}[Y|\mathbf{X}_{\sim ij}])}{V_{\mathbf{X}}[Y]}, \tag{26}$$

where $E_{\mathbf{X}_{\sim ij}}(V_{X_i X_j}[Y|\mathbf{X}_{\sim ij}])$ is the expected variance if all but X_i and X_j are fixed. S_{Tij} is estimated using the equations of Section 3.3, where $\mathbf{C}_i$ and $\mathbf{D}_i$ become $\mathbf{C}_{ij}$ and $\mathbf{D}_{ij}$, respectively. These matrices are obtained by substituting both ith and jth columns in $\mathbf{A}$ and $\mathbf{B}$, in accordance with methods in Homma and Saltelli[46] and Saltelli[47] for considering the variance due to multiple input variables. Table 6 provides values of $\hat{V}A$ and the corresponding standard deviation, for each pair of unknown input variables. Note that the shaking intensity for Y_k^* is the 25% probability of exceedance value in all cases. The largest value of $\hat{V}A$ is obtained for unknown lateral system and age. This makes sense, given that these two variables also produce the largest value of $\hat{V}A$ for one unknown input variable. Similarly, the smallest value of $\hat{V}A$ is obtained for unknown occupancy and nonstructural component quantities, the two variables that produce the smallest values of $\hat{V}A$ for one unknown variable.

Figure 9 shows CDFs of $\hat{Y}_u^{Amp}$ for each pair of unknown $\mathbf{X}_{i,j}$ and shaking intensity with 10% probability of exceedance. $\mathbf{X}_{\sim 1,i,j}$ are fixed at their median values ($\tilde{\mathbf{X}}_{\sim 1,i,j}$). The CDFs of $\hat{Y}_u^{Amp}$ are compared to empirical CDFs of observed Y_u. Also shown are Y_k for each possible combination of unknown $\mathbf{X}_{i,j}$ (only the 1st, 50th, and 99th percentile values are shown for nonstructural component quantities) and $\tilde{\mathbf{X}}_{\sim 1,i,j}$. $\hat{Y}_u^{Amp}$ appears to align well with the observed Y_u, for each unknown $\mathbf{X}_{i,j}$. Equivalent figures for other values of shaking intensity (50%, 20%, and 6% probabilities of exceedance) can be found

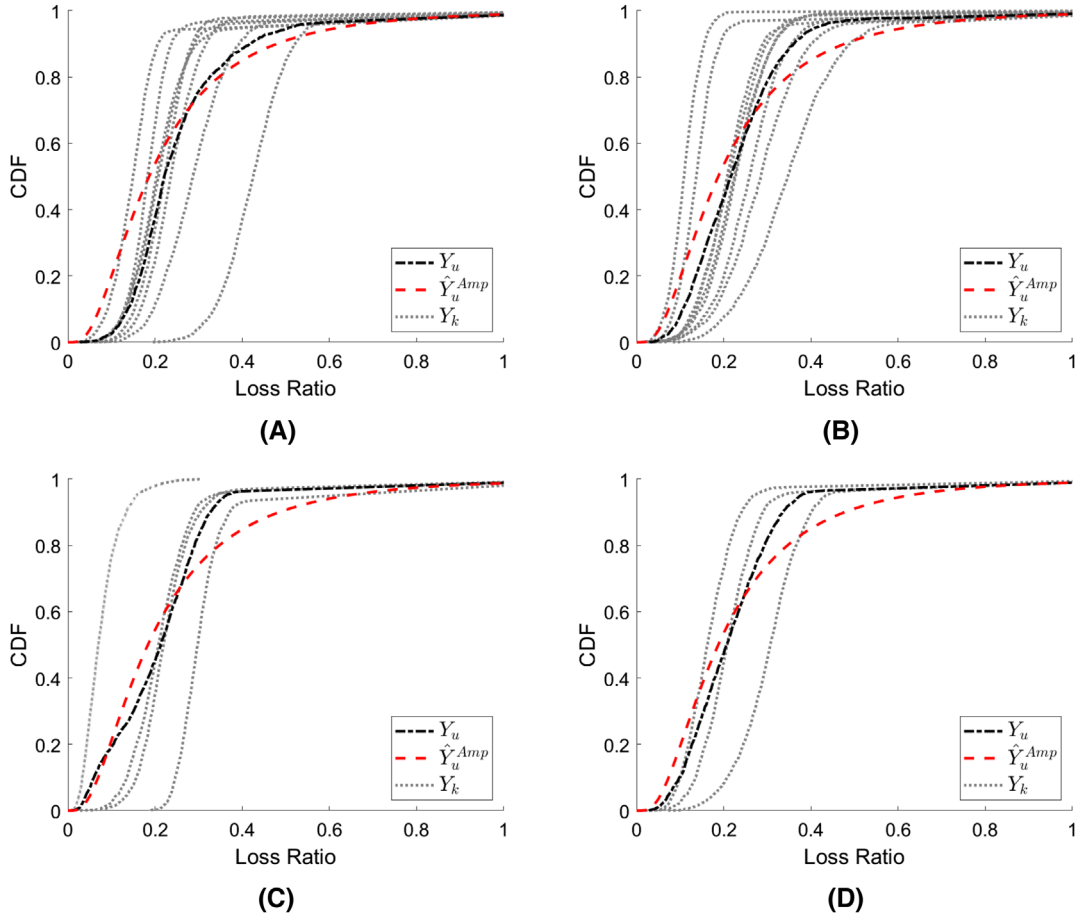

FIGURE 8 Comparison of $\hat{Y}_u^{Amp}$ and observed Y_u when unknown X_i is (A) lateral system, (B) occupancy, (C) age, and (D) nonstructural component quantities, for shaking intensity with 10% probability of exceedance. $\mathbf{X}_{\sim 1,i}$ are fixed at their median values ($\tilde{\mathbf{X}}_{\sim 1,i}$). Also shown are Y_k for each possible fixed value of X_i (only the 1st, 50th, and 99th percentile values are shown for nonstructural component quantities), with $\tilde{\mathbf{X}}_{\sim 1,i}$.

TABLE 6 Uncertainty quantification for pairs of unknown input variables

Unknown input variables	S_{Tij}	$\hat{V}A$	$\sqrt{\hat{V}A}$
Lateral system and occupancy	0.46	0.003	0.06
Lateral system and age	0.64	0.008	0.09
Lateral system and nonstructural quantities	0.48	0.004	0.07
Occupancy and age	0.61	0.008	0.09
Occupancy and nonstructural quantities	0.44	0.003	0.06
Age and nonstructural quantities	0.60	0.007	0.09

in Supporting Information Appendix C. $\hat{Y}_u^{Amp}$ appears to align well with the observed Y_u, for each unknown $\mathbf{X}_{i,j}$ at each of these levels of shaking intensity.

7 | CONCLUSIONS

We have conducted variance-based sensitivity analyses and subsequent uncertainty quantification for loss (i.e., building loss ratio and reoccupancy time) predictions of the FEMA P-58 seismic performance assessment procedure, using a 7-story and a 14-story building at an example site in downtown Los Angeles as case studies. These analyses are important, as

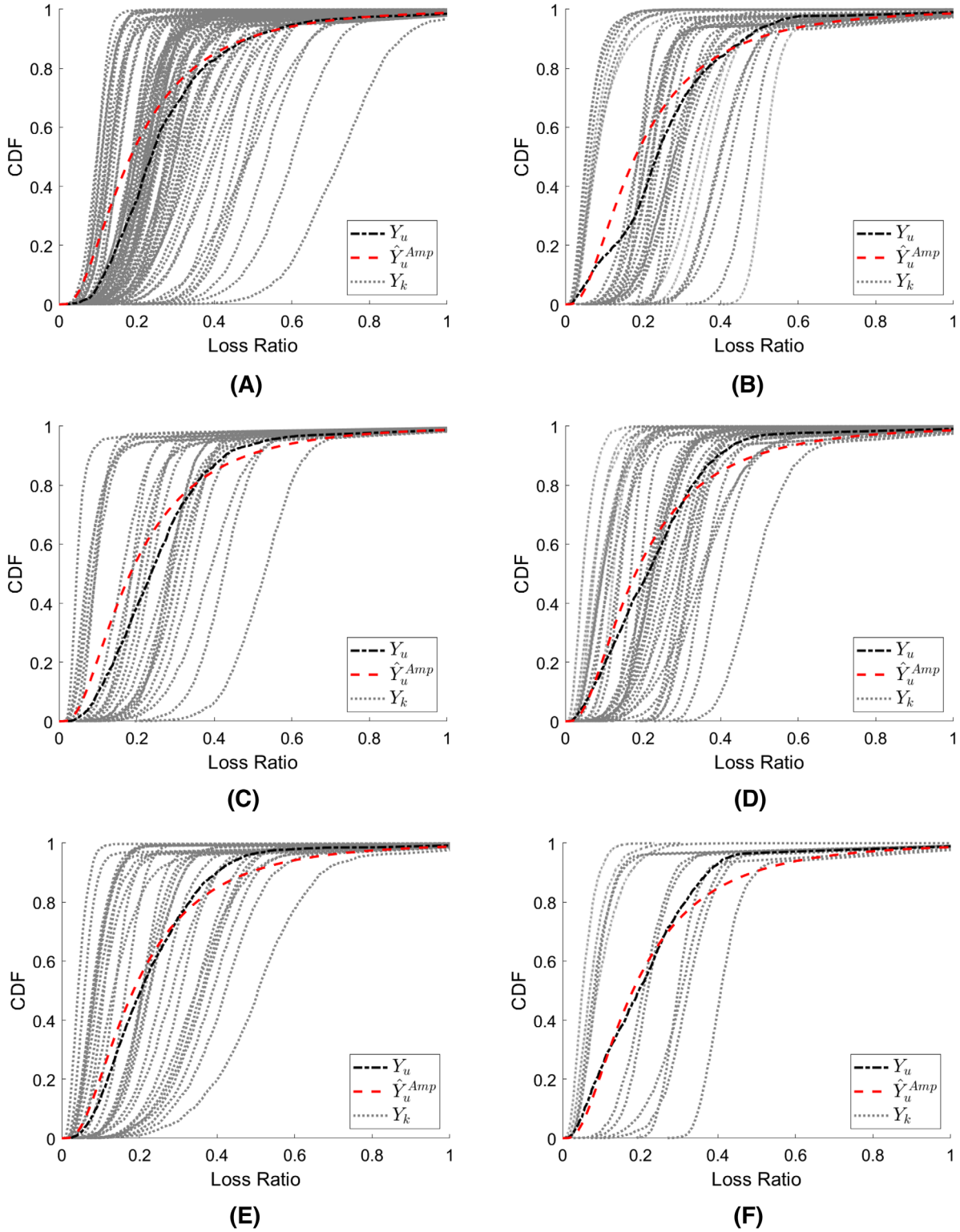

FIGURE 9 Comparison of $\hat{Y}_u^{Amp}$ and observed Y_u when unknown $\mathbf{X}_{i,j}$ are (A) lateral system and occupancy, (B) lateral system and age, (C) lateral system and nonstructural component quantities, (D) occupancy and age, (E) occupancy and nonstructural component quantities, and (F) age and nonstructural component quantities, for shaking intensity with 10% probability of exceedance $\mathbf{X}_{\sim 1,i,j}$ are fixed at their median values ($\tilde{\mathbf{X}}_{\sim 1,i,j}$). Also shown are Y_k for each possible fixed combination of $\mathbf{X}_{i,j}$ (only the 1st, 50th, and 99th percentiles are included for nonstructural component quantities), with $\tilde{\mathbf{X}}_{\sim 1,i,j}$

seismic loss predictions are useful for many different stakeholders but are often calculated using imperfect input information. The popular variance-based approach adopted in this work offers better insight into the importance of variables within a probabilistic seismic performance evaluation than OAT deterministic sensitivity analysis used in a previous similar study.

Results of the sensitivity analyses are very similar for both buildings, indicating that the height of the building does not significantly affect the sensitivities of the loss predictions, at least for the considered cases. Of the six inputs considered in the analyses, building loss ratio predictions are most sensitive to shaking intensity and building age, while reoccupancy time predictions are most sensitive to shaking intensity and lateral system. Calculated sensitivities for building loss ratio were benchmarked using the HAZUS methodology, and a similar trend in sensitivity is observed for the HAZUS loss assessment results. Conclusions of the sensitivity analyses can change however, depending on the level of information known about each input variable. For example, the sensitivity of building loss ratio to lateral system decreases significantly if the building is known to be made of concrete.

Finally, we quantified the predicted additional uncertainty in building loss ratio that results from different inputs being unknown. We found that the largest predicted additional uncertainties in the output were caused by the building's lateral system or age (or both) being unknown. The predicted additional uncertainties were used to estimate an adapted building loss ratio distribution for the unknown model inputs. The adapted building loss ratio distributions align well with the corresponding observed empirical distributions, for all levels of shaking intensity examined.

It is noteworthy that the findings of this study relate to one or two hypothetical buildings, thus the general trends observed in output prediction sensitivity and uncertainty quantification should be verified for additional cases. This work nevertheless provides an important enhanced understanding of the interaction between inputs and consequence predictions of the P-58 methodology.

ACKNOWLEDGMENTS

An academic license of the SP3 software (www.hbrisk.com) was used to perform P-58 analyses, and we thank Katie Wade at HB-Risk for all her assistance with this software.

ORCID

Gemma Cremen https://orcid.org/0000-0002-6699-7312
Jack W. Baker https://orcid.org/0000-0003-2744-9599

REFERENCES

1. Woo G. Natural catastrophe probable maximum loss. *Br Actuar J*. 2002;8:943-959.
2. Dominey-Howes D, Dunbar P, Varner J, Papathoma-Köhle M. Estimating probable maximum loss from a Cascadia tsunami. *Nat Hazard*. 2010;53(1):43-61.
3. Porter KA, Beck JL, Shaikhutdinov R. Simplified estimation of economic seismic risk for buildings. *Earthquake Spectra*. 2004;20(4):1239-1263.
4. Mitchell-Wallace K, Jones M, Hillier J, Foote M. *Natural Catastrophe Risk Management and Modelling: A Practitioner's Guide*. Hoboken. NJ: John Wiley & Sons; 2017.
5. Taylor P. Calculating financial loss from catastrophes. Proceedings of the SECED Conference; July 9–10, 2015; Cambridge, UK.
6. Marsh. *A Decade of Advances In Catastrophe Modeling and Risk Financing*. New York, NY: Marsh LLC; 2015.
7. Michel G. *Risk Modeling for Hazards and Disasters*. Amsterdam: Elsevier; 2017.
8. Tyagunov S, Pittore M, Wieland M, et al. Uncertainty and sensitivity analyses in seismic risk assessments on the example of Cologne, Germany. *Nat Hazards Earth Syst Sci*. 2014;14(6):1625-1640.
9. Dyanati M, Huang Q, Roke D. Sensitivity analysis of seismic performance assessment and consequent impacts on loss analysis. *Bull Earthquake Eng*. 2017;15(11):4751-4790.
10. Lamprou A, Jia G, Taflanidis AA. Life-cycle seismic loss estimation and global sensitivity analysis based on stochastic ground motion modeling. *Eng Struct*. 2013;54:192-206.
11. Porter KA, Beck JL, Shaikhutdinov RV. Sensitivity of building loss estimates to major uncertain variables. *Earthquake Spectra*. 2002;18(4):719-743.
12. FEMA. *FEMA P-58-1: Seismic Performance Assessment of Buildings. Volume 1—Methodology*. Washington, DC: Federal Emergency Management Agency; 2012.
13. Moehle J, Deierlein GG. A framework methodology for performance-based earthquake engineering. 13th World Conference on Earthquake Engineering; August 16, 2004; Vancouver, BC:3812-3814.
14. Borgonovo E, Plischke E. Sensitivity analysis: a review of recent advances. *Eur J Oper Res*. 2016;248(3):869-887.
15. Saltelli A, Tarantola S, Campolongo F, Ratto M. *Sensitivity Analysis in Practice: A Guide to Assessing Scientific Models*. 1. Wiley Online Library; 2004.

16. Papadopoulos AN, Vamvatsikos D, Kazantzi AK. Development and application of FEMA P-58 compatible story loss functions. *Earthquake Spectra*. 2019;35(1):95-112.
17. Oakley JE, O'Hagan A. Probabilistic sensitivity analysis of complex models: a Bayesian approach. *J R Stat Soc Series B Stat Methodol*. 2004;66(3):751-769.
18. Sobol IM. Sensitivity estimates for nonlinear mathematical models. *Mathematical Modelling and Computational Experiments*. 1993;1(4):407-414.
19. Saltelli A, Annoni P, Azzini I, Campolongo F, Ratto M, Tarantola S. Variance based sensitivity analysis of model output. Design and estimator for the total sensitivity index. *Comput Phys Commun*. 2010;181(2):259-270.
20. Jacques J, Lavergne C, Devictor N. Sensitivity analysis in presence of model uncertainty and correlated inputs. *Reliab Eng Syst Saf*. 2006;91(10-11):1126-1134.
21. Haselton Baker Risk Group. Seismic Performance Prediction Program (SP3); 2017. http://www.hbrisk.com.
22. Cook D, Wade K, Haselton CB, Baker JW, DeBock J. A structural response prediction engine to support advanced seismic risk assessment. Eleventh U.S. National Conference on Earthquake Engineering, Los Angeles, CA; 2018.
23. Field EH, Jordan TH, Cornell CA. OpenSHA: a developing community-modeling environment for seismic hazard analysis. *Seismological Research Letters*. 2003;74(4):406-419.
24. FEMA. *Earthquake-Resistant Design Concepts—An Introduction to the NEHRP Recommended Seismic Provisions for New Buildings and Other Structures* [FEMA P-749]. Washington, DC: Federal Emergency Management Agency; 2010. http://www.fema.gov.
25. FEMA. *HAZUS MH-2.1 Earthquake Model Technical Manual*. Washington, DC: Federal Emergency Management Agency; 2015.
26. Goel RK, Chopra AK. Period formulas for concrete shear wall buildings. *J Struct Eng*. 1998;124(4):426-433.
27. Goel RK, Chopra AK. Period formulas for moment-resisting frame buildings. *J Struct Eng*. 1997;123(11):1454-1461.
28. Gilles D, McClure G, Chouinard LE. Uncertainty in fundamental period estimates leads to inaccurate design seismic loads. *Can J Civ Eng*. 2011;38(8):870-880.
29. FEMA. *NEHRP Recommended Provisions for Seismic Regulations for New Buildings and Other Structures: Provisions*. Vol. 302. BSSC Program on Improved Seismic Safety Provisions; 1997.
30. Petersen MD, Frankel AD, Harmsen SC, et al. *Documentation for the 2008 Update of the United States National Seismic Hazard Maps* [Open-File Report 2008-1128, Technical Report]. Reston, VA: United States Geological Survey; 2008.
31. Pacific Coast Building Officials' Conference. *Uniform Building Code*. Pacific Coast Building Officials' Conference; 1935.
32. Pacific Coast Building Officials' Conference. *Uniform Building Code*. Pacific Coast Building Officials' Conference; 1955.
33. International Conference of Building Officials. *Uniform Building Code*. International Conference of Building Officials; 1976.
34. ASCE. *Minimum Design Loads for Buildings and Other Structures, ASCE/SEI 7-10*. Reston, VA: American Society of Civil Engineers; 2010.
35. Fierro EA, Reitherman R. *Reducing the Risks of Nonstructural Earthquake Damage: A Practical Guide*. Darby, PA: DIANE Publishing; 1995.
36. FEMA. *FEMA P-58-3: Seismic Performance Assessment of Buildings. Peformance Assessment Calculation Tool (PACT)*. Vol. 3. Washington, DC: Federal Emergency Management Agency; 2012.
37. Almufti I, Willford M. *Resilience-Based Earthquake Design (REDi) Rating System, Version 1.0*. London: Arup; 2013. https://www.arup.com/perspectives/publications/research/section/redi-rating-system.
38. Saint-Geours N, Bailly JS, Lavergne C, Grelot F. Latin hypercube sampling of Gaussian random field for Sobol' global sensitivity analysis of models with spatial inputs and scalar output. HAL-Inria; 2010:81-84.
39. Yun W, Lu Z, Zhang K, Jiang X. An efficient sampling method for variance-based sensitivity analysis. *Struct Saf*. 2017;65:74-83.
40. Archer G, Saltelli A, Sobol I. Sensitivity measures, ANOVA-like techniques and the use of bootstrap. *J Stat Comput Simul*. 1997;58(2):99-120.
41. Baio G, Dawid AP. Probabilistic sensitivity analysis in health economics. *Stat Methods Med Res*. 2015;24(6):615-634.
42. Saltelli A, Annoni P. How to avoid a perfunctory sensitivity analysis. *Environ Model Softw*. 2010;25(12):1508-1517.
43. Ades A, Claxton K, Sculpher M. Evidence synthesis, parameter correlation and probabilistic sensitivity analysis. *Health Econ*. 2006;15(4):373-381.
44. Smith AE, Ryan PB, Evans JS. The effect of neglecting correlations when propagating uncertainty and estimating the population distribution of risk. *Risk Anal*. 1992;12(4):467-474.
45. Christopher Frey H, Patil SR. Identification and review of sensitivity analysis methods. *Risk Anal*. 2002;22(3):553-578.
46. Homma T, Saltelli A. Importance measures in global sensitivity analysis of nonlinear models. *Reliab Eng Syst Saf*. 1996;52(1):1-17.
47. Saltelli A. Making best use of model evaluations to compute sensitivity indices. *Comput Phys Commun*. 2002;145(2):280-297.

SUPPORTING INFORMATION

Additional supporting information may be found online in the Supporting Information section at the end of the article.

How to cite this article: Cremen G, Baker JW. Variance-based sensitivity analyses and uncertainty quantification for FEMA P-58 consequence predictions. *Earthquake Engng Struct Dyn*. 2020;1-20. https://doi.org/10.1002/eqe.3370